Hindawi Publishing Corporation
Journal of Nanomaterials
Volume 2015, Article ID 182691, 6 pages
http://dx.doi.org/10.1155/2015/182691

Research Article

YIG: Bi_2O_3 Nanocomposite Thin Films for Magnetooptic and Microwave Applications

M. Nur-E-Alam,[1] Mikhail Vasiliev,[1] Kamal Alameh,[1] Viacheslav Kotov,[2] Victor Demidov,[2] and Dmitry Balabanov[3]

[1]*Electron Science Research Institute, Edith Cowan University, 270 Joondalup Drive, Joondalup, WA 6027, Australia*
[2]*Institute of Radio Engineering and Electronics, RAS, 11 Mokhovaya Street, Moscow 125009, Russia*
[3]*Moscow Institute of Physics and Technology, 9 Institutskiy Pereulok, Dolgoprudny, Moscow Region 141700, Russia*

Correspondence should be addressed to M. Nur-E-Alam; m.nur-e-alam@ecu.edu.au

Received 14 April 2015; Accepted 14 June 2015

Academic Editor: Christian Brosseau

$Y_3Fe_5O_{12}$-Bi_2O_3 composite thin films are deposited onto $Gd_3Ga_5O_{12}$ (GGG) substrates and their annealing crystallization regimes are optimized (in terms of both process temperatures and durations) to obtain high-quality thin film layers possessing magnetic properties attractive for a range of technological applications. The amount of bismuth oxide content introduced into these nanocomposite-type films is controlled by adjusting the RF power densities applied to both $Y_3Fe_5O_{12}$ and Bi_2O_3 sputtering targets during the cosputtering deposition processes. The measured material properties of oven-annealed YIG-Bi_2O_3 films indicate that cosputtering of YIG-Bi_2O_3 composites can provide the flexibility of application-specific YIG layers fabrication of interest for several existing, emerging, and also frontier technologies. Experimental results demonstrate large specific Faraday rotation (of more than $1^\circ/\mu$m at 532 nm), achieved simultaneously with low optical losses in the visible range and very narrow peak-to-peak ferromagnetic resonance linewidth of around $\Delta H_{pp} = 6.1$ Oe at 9.77 GHz.

1. Introduction

$Y_3Fe_5O_{12}$ (YIG) is one of the most widely known ferrimagnetic garnet crystals among all rare-earth iron garnets due to its strong application potential in the fields of optics, magnetooptics (MO), and microwave devices. YIG is a very common material used in various microwave-range and optical devices such as circulators, isolators, filters, and switches [1–5]. A significant number of research works have been conducted worldwide by many researchers to synthesize YIG thin films using various thin film deposition techniques, and their various magnetic and microwave properties have been reported extensively [1–15]. To achieve further improvements in their properties, some work has been conducted recently to deposit thin films of YIG whilst slightly varying their compositional stoichiometry [16–19]. Among all YIG thin-film fabrication techniques, radio frequency (RF) magnetron sputtering is more effective than other physical vapor deposition methods, mainly due to the relative simplicity of process, strong potential for process industrialization, and the superior thin-film quality obtainable with RF sputtering. YIG thin films do not possess giant Faraday rotation in the visible or near-infrared ranges, and their microstructural properties depend strongly on the substrate type, since they require high-temperature postdeposition annealing processes (run at around 700–740°C) for the formation of garnet-phase layers. Several successful attempts at YIG synthesis have been reported using various substrate types such as Si, metal, and quartz to improve their magnetic and microstructural properties and especially to avoid microcrack formation due to high-temperature annealing treatment [1].

In this work, we prepare several batches of YIG-bismuth oxide composite thin films using RF magnetron cosputtering, optimize the amount of excess bismuth oxide content added to the film layer volumes, fine-tune the deposition conditions, and study the effects of various process parameters on the magnetic and magnetooptic properties of film layers. We also optimize the annealing regimes suitable for the

crystallization of cosputtered $(Y,Bi)_3Fe_5O_{12}$-Bi_2O_3 thin films, in order to obtain good surface quality together with attractive magnetic properties (as evidenced by the appearance of strong Faraday rotation in the visible range) without inducing microcracks. Experimental results demonstrate the possibility of annealing these nanocomposite thin films using relatively low process temperatures (near 600°C) and short crystallization process durations. The goal of this work is to provide good quality composition-adjusted YIG-type thin films with high specific Faraday rotation, high MO figure of merit in the visible range, and to achieve simultaneously a rather narrow ferromagnetic resonance (FMR) linewidth, which is of significant interest for various modern MO and microwave applications and technologies. We pay special attention to controlling multiple film parameters of importance, the film thickness, optical absorption spectra, specific Faraday rotation, and magnetization vector direction, while synthesizing a range of YIG-Bi_2O_3 nanocomposite materials as all of these properties are crucial for the development of new advanced functional materials for use in many emerging integrated optics, photonics, and microwave applications. The fabrication processes, their details, and some film characterization results are described in Section 2; the summary of results achieved during our experimental work on the synthesis of high-performance optimized-composition nanocomposite layers of $(Y,Bi)_3Fe_5O_{12}$-Bi_2O_3 is discussed and analyzed in Section 3. Finally, we draw a conclusion in Section 4.

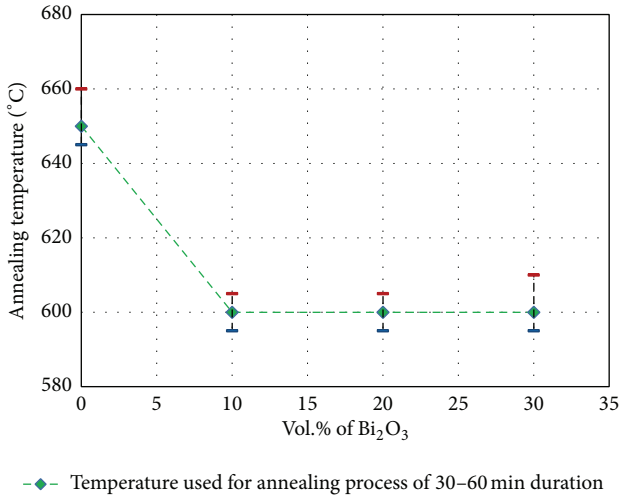

Figure 1: A summary of optimized annealing regimes used to crystallize the stoichiometric YIG and also YIG-Bi_2O_3 thin films showing the upper and lower annealing temperature limits. The most suitable annealing temperatures for each batch of samples were found by running several annealing trials for each batch whilst varying the process durations between 30 minutes and 3 hours, followed by measurements of specific Faraday rotation; we found that the best annealing durations for these film types were between 30 and 60 minutes.

2. Growth and Characterization of YIG: Bi_2O_3 Cosputtered Composite Layers

YIG and YIG-Bi_2O_3 (with up to 30 vol.% of added cosputtered bismuth oxide content) films (of thickness between 100 and 1000 nm) were deposited by RF sputtering or cosputtering onto chemically and ultrasonically cleaned gadolinium gallium garnet (GGG (111)) substrates from two separate oxide (Bi_2O_3) and oxide-mix-based ($Y_3Fe_5O_{12}$) ceramic targets. The material purity levels in all target materials were in excess of 99.99%. The sputtering conditions and process parameters such as process gas (Ar) pressure and RF power density were optimized for each of the individual sputtering targets and also for running the cosputtering processes. The deposition runs used to synthesize the YIG and YIG-Bi_2O_3 films were performed at vacuum base pressure of about $P_{(\text{base})} < 1\text{-}2E-06$ Torr (high vacuum) and at argon gas pressure of about $P(\text{Ar}) \approx 2\text{-}3$ mTorr; we used 3-inch diameter targets placed approximately 18 cm away from the center of rotating substrate stage kept at room temperature. The process gas was pure Ar and no oxygen input was used. The volumetric fraction of Bi_2O_3 content added to the YIG during the deposition processes was controlled by the adjustments of RF power densities applied to the sputtering targets, and the percentages of added bismuth oxide content were calculated using their partial deposition rates according to the methodologies described in [20]. The deposition rates for the stoichiometric YIG and also for the cosputtered films were monitored in situ in real time during the deposition processes using a quartz microbalance sensor and the film thicknesses were determined from the quartz sensor information after running multiple calibration runs for determining the precise tooling factors. The as-deposited YIG layers and YIG-Bi_2O_3 composite layers (amorphous in phase immediately after deposition, as evidenced by the absence of any measurable magnetic properties) were crystallized by using oven-annealing processes, which were optimized for each material type by running multiple annealing trials including multistep annealing processes, which were followed by Faraday rotation measurements to confirm the formation of garnet phase. A relatively higher temperature is required to anneal the nominally stoichiometric YIG layers (at least 650°C in our air-atmosphere annealing experiments) compared with the YIG-Bi_2O_3 nanocomposites. However, we managed to establish a common optimized annealing regime (30 minutes at 600°C) suitable for the crystallization of all YIG-Bi_2O_3 film materials trialled. Figure 1 shows the summary of the annealing regimes that were used to successfully anneal all of the YIG and YIG-Bi_2O_3 thin film materials sputtered onto GGG substrates (which was confirmed by the appearance of measurable Faraday rotation in films possessing smooth surfaces without any signs of thermal decomposition). Some of the already-annealed films were subsequently reannealed at a slightly higher temperature and at a longer time duration to check if this reannealing process would alter their MO properties (specific Faraday rotation) or optical transmission spectra, and typically no subsequent improvements or changes in their MO properties were observed. The crystallized (suitably annealed, as judged by the largest-obtained specific Faraday

rotations measured at 532 nm) YIG and YIG-Bi_2O_3 nanocrystalline films were characterized using a Beckman Coulter DU 640B UV/Visible spectrophotometer, Thorlabs PAX polarimeter system used in conjunction with a custom-made calibrated electromagnet, and several of the nanocomposite films were also subjected to measurements of their ferromagnetic resonance (FMR) linewidth. The FMR measurements were conducted at the Institute of Radio Engineering and Electronics, Russian Academy of Sciences. Using specialized thickness-fitting software (a customized software package for thin-film characterization developed at Edith Cowan University, Australia, which uses the spectrally fitted transmission curves and complex refractive index dispersion data to derive the fitted film thickness [20, 21]), the thicknesses of all YIG and YIG-Bi_2O_3 films were reconfirmed after annealing, and we found that the estimated thickness measurement accuracy was within about ±2%. The microstructural properties of YIG and YIG-Bi_2O_3 thin films were investigated by making the X-ray diffraction (XRD) measurements using Siemens D 5000 X-ray diffractometer.

3. Properties of $Y_3Fe_5O_{12}$-Bi_2O_3 Composite Thin Films, Analysis, and Discussion

The annealed adjusted-stoichiometry YIG ($(YBi)_3Fe_5O_{12}$) films exhibited a rather high specific Faraday rotation at 532 nm, compared to typical stoichiometric YIG films sputtered from the same target, which also required annealing at higher temperatures near at least 650°C. These factors suggest strongly that partial bismuth substitution of YIG did occur as a result of bismuth atoms being able to occupy the dodecahedral sublattice sites within the crystal structure of garnet, substituting some of the yttrium atoms. Moreover, the specific Faraday rotation values were found to increase with increasing the volumetric content of Bi_2O_3 added to composites during the deposition process (the measured specific Faraday rotation data for several $Y_3Fe_5O_{12}$-Bi_2O_3 composition types are shown in Figure 2).

According to the data reported in literature [22], the specific Faraday rotation of epitaxially grown pure YIG at 300 K is near 0.08°/μm at 635 nm and 0.3°/μm at 532 nm. Smaller values of Faraday rotation obtained indicate that parts of the film's volume were in an amorphous state. The measured MO figures of merit (defined as the doubled ratio of specific Faraday rotation to the optical absorption coefficient at the same wavelength, that is, $Q = 2 * |\Theta_F|/\alpha$, where α is the optical absorption coefficient) increased with the amount of added Bi_2O_3 content because of the lower optical losses in the composite films [21, 23], which had higher visible-range transmission. The lower optical losses in oxide-mixed films can be attributed to the high transparency of bismuth oxide which is very likely present in regions surrounding the grains of garnet, yet this is difficult to confirm conclusively using XRD data, unless some volume of any crystallized Bi_2O_3 phases also forms within films. The highest MO figure of merit was about 3.9° at 532 nm, measured in a composite film of composition-type YIG-Bi_2O_3 (30 vol.%), which was annealed at 600°C for 30 minutes. The absorption spectra for the annealed composites were derived using a software-assisted procedure based on iterative fitting of the spectral features observed in the measured and modeled transmission spectra of the films (the details of this procedure were reported in [21]). All of the annealed garnet-type composite films showed a significantly high remnant magnetization, observed during the measurements of specific Faraday rotation, which indicated that these films had a strong uniaxial magnetic anisotropy. Table 1 summarizes the measured absorption coefficients and the MO figures of merit for several stoichiometric types of YIG-Bi_2O_3 films at 532 and 635 nm.

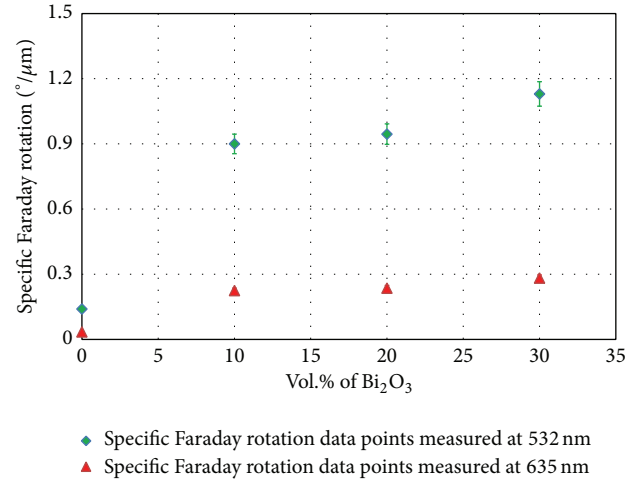

Figure 2: Measured specific Faraday rotation data points of annealed YIG thin films and different $Y_3Fe_5O_{12}$-Bi_2O_3 nanocomposite thin films. The specific Faraday rotation measurements for all samples were performed using a 532 nm polarized light source and a custom-made electromagnet used in conjunction with Thorlabs PAX polarimeter system.

XRD measurements were performed by using detector-arm scanning technique in theta-theta diffractometer configuration, at near-grazing X-ray radiation incidence, and for the range of 2θ angles between 25° and 65°. Cu Kα_1 radiation line was used, and a diffracted-beam collimator was used in the detector arm. The X-ray diffraction datasets obtained from YIG and YIG-Bi_2O_3 film samples and pattern indexing information are shown in Figure 3. The positions of the X-ray diffraction peaks obtained from all samples were determined by using the peak-listing options of Jade 9 (MDI Corp.) software. Compared to the XRD spectra for $(Er,Y)_3Fe_5O_{12}$ thin films reported by Shaiboub et al. [24], the XRD peaks dataset obtained in our experiment suggests that we were able to deposit and anneal YIG and YIG-Bi_2O_3 composite layers. The presence of single phase with the diffraction lines (*hkl*) in optimized anneal samples resulted in the cubic garnet structure. The strongest peaks belonging to (420) observed for YIG-Bi_2O_3 (10 and 30 vol.%) composite layers at the 2θ (°) values of 32.516 and 32.656 correspond with the *d*-spacing values of 2.751 and 2.739 Å, respectively, indicating the formation of cubic garnet single phase of possible bismuth-doped yttrium iron garnet layers [25]. On the other hand in composite layer YIG-Bi_2O_3

Table 1: Derived optical absorption coefficients and the calculated MO figures of merit for YIG and YIG-Bi_2O_3 composite thin films prepared on GGG substrates.

Material composition type	Absorption coefficient (cm^{-1}) at 532 nm	MO figure of merit (deg.) at 532 nm	Absorption coefficient (cm^{-1}) at 635 nm	MO figure of merit (deg.) at 635 nm
$Y_3Fe_5O_{12}$	12342	0.22	7986	0.08
$Y_3Fe_5O_{12}$ + Bi_2O_3 (10 vol.%)	7965	2.41	3044	1.48
$Y_3Fe_5O_{12}$ + Bi_2O_3 (20 vol.%)	6607	3.05	2822	1.67
$Y_3Fe_5O_{12}$ + Bi_2O_3 (30 vol.%)	6072	3.96	2449	2.30

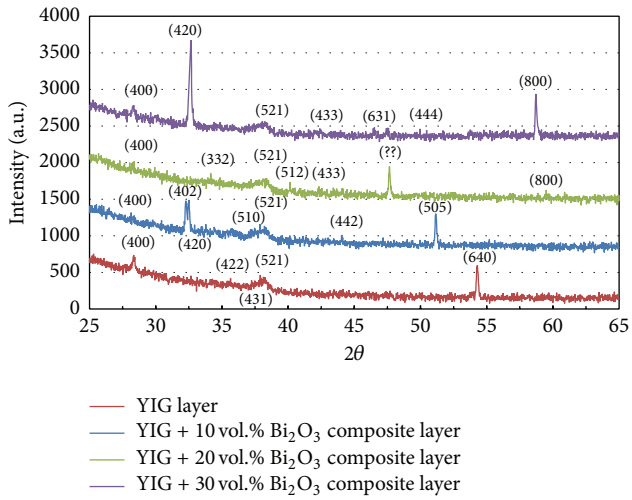

Figure 3: X-ray diffraction datasets obtained from YIG and YIG: Bi_2O_3 composite film layers.

(20 vol.%), the peak (420) was not observed; however, the other observed garnet peaks had a nonidentifiable strong peak at 47.659°, which represents foreign material contamination that occurred during the sample preparation. Whilst the XRD traces measured in different sample types did not show exactly the same diffracted peak detection patterns, all peaks identified within our indexed patterns had even sums of their Miller indices, confirming the body-centered cubic lattice-type characteristic of magnetic garnets. According to [26], in crystalline materials of this lattice type, the reflections with even sums of Miller indices are possibly present yet are not present necessarily; the latter can be related to the lattice-strain-induced displacements of individual atoms within the unit cell structure. We believe that the presence of amorphous Bi_2O_3 phase in-between the crystallized grains of garnet could lead to the observed inconsistencies in the detected X-ray diffraction peaks.

The cubic lattice parameters were calculated from the combination of Bragg's equation and d-spacing expression using the following formula:

$$a = \left[\frac{\lambda^2\left(h^2 + k^2 + l^2\right)}{4\sin^2\theta}\right]^{1/2}, \quad (1)$$

where λ is the wavelength of Cu Kα_1 radiation and θ is the diffracted-beam peak angle of a peak corresponding to any identified Miller index combination (hkl).

Table 2: Calculated average lattice constant and crystallite size of YIG and YIG-Bi_2O_3 composite thin films prepared on GGG substrates.

Material composition type	Average lattice constant (Å)	Average crystallite size (nm)
$Y_3Fe_5O_{12}$	12.37	27
$Y_3Fe_5O_{12}$ + Bi_2O_3 (10 vol.%)	12.48	35
$Y_3Fe_5O_{12}$ + Bi_2O_3 (20 vol.%)	12.45	36
$Y_3Fe_5O_{12}$ + Bi_2O_3 (30 vol.%)	12.49	42

The average crystallite size was calculated according to Scherrer's equation, $D = k\lambda/\beta\cos\theta$, where D is the mean crystallite size, k (0.94) is Scherrer constant, λ is X-ray wavelength (0.154056 nm), and β is the angular full width at half maximum (FWHM) of the diffraction peaks. The calculated (averaged using data from several identifiable peaks substituted into (1)) lattice constants and (average) crystallite size of crystallized YIG and YIG-Bi_2O_3 layers are detailed in Table 2.

Figure 4 shows the FMR signal trace (recorded in arbitrary units) for a composite sample of composition-type YIG-Bi_2O_3 (20 vol.%) in the film layer of about 500 nm thickness. The FMR measurements were performed at 9.77 GHz and plotted as a function of magnetic field strength. The measured FMR linewidth (calculated considering the full peak-to-peak resonance width) for our YIG-Bi_2O_3 nanocomposite film was 6.1 Oe, which is significantly narrower than FMR linewidth reported recently in YIG layers grown on YAG by pulsed laser deposition [5] and over 10 times narrower than that reported in zirconium-doped yttrium iron garnet prepared by conventional solid-state reaction [19].

We were therefore able to produce a nanocomposite material consisting of $(YBi)_3Fe_5O_{12}$ MO garnet nanocrystals diluted within a dielectric matrix (containing residual amorphous Bi_2O_3 and possibly also some amount of iron and yttrium oxides), which possessed a rather small Bi^{3+} substitution level and (remarkably) an extremely narrow FMR linewidth. We believe that the main reason for this small FMR linewidth was the phase transformation of a polycrystalline material to a nanocomposite material with isolated nanosized garnet grains. These films can be useful for the development of a new class of MO ultrahigh frequency (UHF) modulators based on the interaction of infrared light waveguide modes with magnetostatic waves due to the small optical absorption of infrared light and better temperature stability of our RF-sputtered films when compared with existing sputtered

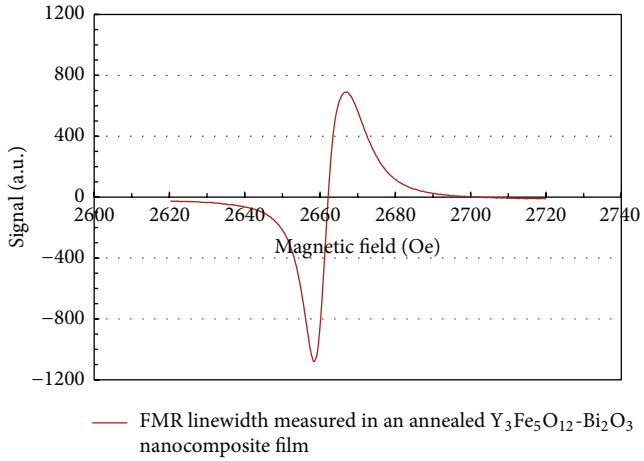

FIGURE 4: Measured FMR behavior and linewidth (ΔH_{pp} = 6.1 Oe at 9.77 GHz) in an annealed $Y_3Fe_5O_{12}$-Bi_2O_3 nanocomposite film of thickness 500 nm sputtered onto a GGG substrate.

and also PLD-synthesized $Bi_3Fe_5O_{12}$ films which usually demonstrated extremely high optical absorption.

The experimental results reported in this paper demonstrate the feasibility of synthesizing new garnet-type nanocomposite functional materials and engineering their magnetic properties, thus making them attractive for many emerging applications in integrated optics, magnetophotonics, and microwave technology.

4. Conclusion

Various RF magnetron cosputtered ($Y_3Fe_5O_{12}$-Bi_2O_3) nanocomposite thin film materials have been prepared. An optimized 500 nm thick composite sample of composition-type YIG-Bi_2O_3 (20 vol.%) has exhibited rather interesting MO properties simultaneously with unusual electromagnetic behavior (an extremely small FMR linewidth of only 6.1 Oe at 9.77 GHz), which is of interest for microwave-range applications. Experimental results have also shown that this new class of YIG-type garnet nanocomposites can provide important ferrimagnetic functional materials for optics, MO, and microwave devices. The methods of synthesizing optimized YIG-bismuth oxide ($Y_3Fe_5O_{12}$-Bi_2O_3) compositions using RF magnetron cosputtering processes followed by postdeposition air-atmosphere oven-annealing have been described in detail.

Conflict of Interests

The authors declare no conflict of interests.

Acknowledgments

This research is supported by Electron Science Research Institute, Faculty of Health, Engineering and Science (FHES), Edith Cowan University, Australia, and BFBR Grants 12-07-00502, 13-07-00418, 13-07-00242, 13-07-12056, and 13-07-12404.

References

[1] Y. Y. Sun, Y.-Y. Song, and M. Wu, "Growth and ferromagnetic resonance of yttrium iron garnet thin films on metals," *Applied Physics Letters*, vol. 101, no. 8, Article ID 082405, 2012.

[2] S. A. Manuilov and A. M. Grishin, "Pulsed laser deposited $Y_3Fe_5O_{12}$ films: nature of magnetic anisotropy II," *Journal of Applied Physics*, vol. 108, no. 1, Article ID 013902, 2010.

[3] S. E. Irvine and A. Y. Elezzabi, "Wideband magneto-optic modulation in a bismuth-substituted yttrium iron garnet waveguide," *Optics Communications*, vol. 220, no. 4–6, pp. 325–329, 2003.

[4] R. Marcelli, P. De Gasperis, M. C. Martucci et al., "Growth by rf sputtering and characterization of magnetic garnet films," *Journal of Magnetism and Magnetic Materials*, vol. 104–107, no. 1, pp. 436–438, 1992.

[5] A. Sposito, T. C. May-Smith, G. B. G. Stenning, P. A. J. de Groot, and R. W. Eason, "Pulsed laser deposition of high-quality μm-thick YIG films on YAG," *Optical Materials Express*, vol. 3, no. 5, pp. 624–632, 2013.

[6] W.-C. Chiang, M. Y. Chern, J. G. Lin, and C. Y. Huang, "FMR studies of $Y_3Fe_5O_{12}/Gd_3Ga_5O_{12}$ (YIG/GGG) superlattices and YIG thin films," *Journal of Magnetism and Magnetic Materials*, vol. 239, no. 1-3, pp. 332–334, 2002.

[7] Z. Abbas, R. M. Al-Habashi, K. Khalid, and M. Maarof, "Garnet ferrite ($Y_3Fe_5O_{12}$) nanoparticles prepared via modified conventional mixing oxides (MCMO) method," *European Journal of Scientific Research*, vol. 36, no. 2, pp. 154–160, 2009.

[8] Y. Sun, Y. Y. Song, H. Chang et al., "Growth and ferromagnetic resonance properties of nanometer-thick yttrium iron garnet films," *Applied Physics Letters*, vol. 101, no. 15, Article ID 152405, 2012.

[9] B. A. Samad, M. F. Blanc-Mignon, M. Roumie, A. Siblini, J. P. Chatelon, and M. Korek, "Physico-chemical characterization of multilayer YIG thin film deposited by rf sputtering," *The European Physical Journal Applied Physics*, vol. 50, no. 1, Article ID 10502, 2010.

[10] T. Nakano, H. Yuri, and U. Kihara, "Magneto-optical properties of YIG single crystal by TSFZ method," *IEEE Transactions on Magnetics*, vol. 20, no. 5, pp. 986–988, 1984.

[11] N. Nasir, N. Yahya, M. Kashif et al., "Observation of a cubical-like microstructure of strontium iron garnet and yttrium iron garnet prepared via sol-gel technique," *Journal of Nanoscience and Nanotechnology*, vol. 11, no. 3, pp. 2551–2554, 2011.

[12] S. Kahl and A. M. Grishin, "Pulsed laser deposition of $Y_3Fe_5O_{12}$ and $Bi_3Fe_5O_{12}$ films on garnet substrates," *Journal of Applied Physics*, vol. 93, no. 10, pp. 6945–6947, 2003.

[13] S. Y. Sung, X. Qi, S. K. Mondal, B. J. H. Stadler, and S. Y. Sung, "Partial pressure differential and rapid thermal annealing for integrated yttrium iron garnet (YIG)," *Materials Research Society Symposium—Proceedings*, vol. 817, pp. 213–218, 2004.

[14] S. Yamamoto, H. Kuniki, H. Kurisu, M. Matsuura, and P. Jang, "Post-annealing effect of YIG ferrite thin-films epitaxially grown by reactive sputtering," *Physica Status Solidi A: Applied Research*, vol. 201, no. 8, pp. 1810–1814, 2004.

[15] T. Kim, S. Nasu, and M. Shima, "Growth and magnetic behavior of bismuth substituted yttrium iron garnet nanoparticles," *Journal of Nanoparticle Research*, vol. 9, no. 5, pp. 737–743, 2007.

[16] Y. Mizoguchi, M. Kagawa, Y. Syono, and T. Hirai, "Film synthesis of $Y_3Al_5O_{12}$ and $Y_3Fe_5O_{12}$ by the spray-inductively coupled plasma technique," *Journal of the American Ceramic Society*, vol. 84, no. 3, pp. 651–653, 2001.

[17] R. G. Vidhate, V. D. Murumkar, R. G. Dorik, N. M. Makne, S. R. Nimbore, and K. M. Jadhav, "Magnetic properties of In^{3+} substituted Yttrium iron garnet (YIG)," *Review of Research*, vol. 1, no. 9, pp. 1–4, 2012.

[18] Q.-H. Yang, H.-W. Zhang, Q.-Y. Wen, and Y.-L. Liu, "Effects of off-stoichiometry and density on the magnetic and magneto-optical properties of yttrium iron garnet films by magnetron sputtering method," *Journal of Applied Physics*, vol. 108, no. 7, Article ID 073901, 2010.

[19] J. Wang, Y. Jin, J. Yang, Y. Huang, and T. Qiu, "Effect of ZrO_2 addition on the microstructure and electromagnetic properties of YIG," *Journal of Alloys and Compounds*, vol. 509, no. 19, pp. 5853–5857, 2011.

[20] A. Mohammad, *High performance magneto-optic garnet materials for integrated optics and photonics [Doctoral Thesis]*, Theses: Doctorates and Masters, Paper 528, 2012, http://ro.ecu.edu.au/theses/528.

[21] M. Vasiliev, M. Nur-E-Alam, V. A. Kotov et al., "RF magnetron sputtered $(BiDy)_3(FeGa)_5O_{12}$:Bi_2O_3 composite garnet-oxide materials possessing record magneto-optic quality in the visible spectral region," *Optics Express*, vol. 17, no. 22, pp. 19519–19535, 2009.

[22] P. Hansen and J.-P. Krumme, "Magnetic and magneto-optical properties of garnet films," *Thin Solid Films*, vol. 114, no. 1-2, pp. 69–107, 1984.

[23] M. Nur-E-Alam, M. Vasiliev, V. Kotov, and K. Alameh, "Recent developments in magneto-optic Garnet-type thin-film materials synthesis," *Procedia Engineering*, vol. 76, pp. 61–73, 2014.

[24] R. Shaiboub, N. B. Ibrahim, M. Abdullah, and F. Abdulhade, "The physical properties of Erbium-doped yttrium iron garnet films prepared by sol-gel method," *Journal of Nanomaterials*, vol. 2012, Article ID 524903, 5 pages, 2012.

[25] J. Pigošová, A. Cigáň, and J. Maňka, "Thermal synthesis of bismuth-doped Yttrium iron garnet for magneto-optical imaging," *Measurement Science Review*, vol. 8, no. 5, pp. 126–128, 2008.

[26] B. D. Cullity, *Elements of X-Ray Diffraction*, section 4.6, Addison-Wesley Publishing, Boston, Mass, USA, 2nd edition, 1978.